

# Shunt peaking in neural membranes

Francisco J. H. Heras<sup>1</sup>, Simon B. Laughlin<sup>1</sup>, and Jeremy E. Niven<sup>2</sup>

<sup>1</sup>Department of Zoology, University of Cambridge, Cambridge CB2 3EJ, UK

<sup>2</sup>School of Life Sciences, University of Sussex, Falmer, Brighton BN1 9QG, UK

September 3, 2016

## Abstract

Capacitance limits the bandwidth of engineered and biological electrical circuits because it determines the gain-bandwidth product (GBWP). With a fixed GBWP, bandwidth can only be improved by decreasing gain. In engineered circuits, an inductance reduces this limitation through shunt peaking but no equivalent mechanism has been reported for biological circuits. We show that in blowfly photoreceptors a voltage-dependent  $K^+$  conductance, the fast delayed rectifier (FDR), produces shunt peaking thereby increasing bandwidth without reducing gain. Furthermore, the FDR's time constant is close to the value that maximizes the photoreceptor GBWP whilst reducing distortion associated with the creation of a wide-band filter. Using a model of the honeybee drone photoreceptor, we also show that a voltage-dependent  $Na^+$  conductance can produce shunt peaking if the inactivation time constant is increased. We argue that shunt peaking may be widespread in graded neurons and dendrites.

## 1 Introduction

Like their engineered counterparts, neurons must achieve sufficient bandwidth to transmit fast signals and sufficient gain to prevent noise from corrupting signals. However, a neuron's membrane has the passive electrical properties of an RC parallel circuit [1] with gain  $R$ , and 3dB bandwidth  $1/2\pi RC$ . Thus, the gain-bandwidth product (GBWP) is  $1/2\pi C$ , making capacitance the sole constraint. So, when ion channels change membrane resistance, they trade bandwidth for gain. A membrane's specific capacitance is relatively invariant [2] and there are limits to reducing membrane area [3]. Consequently, membrane capacitance constrains bandwidth at a given gain, and gain at a given bandwidth.

The GBWP of electronic amplifiers is similarly constrained by unavoidable capacitances [4]. The usual means of improving bandwidth without sacrificing gain is miniaturization [5] but there are others. One is shunt peaking; the improvement of the GBWP through the addition of inductive elements [6].

Neural membranes cannot produce sufficiently large electromagnetic inductive effects [7] but they do contain voltage-dependent ion channels that act like inductances by changing their conductance with membrane potential after a delay [8, 9, 10]. These inductive-like effects interact with membrane capacitance to produce resonant neural membranes [1] but their effects on the GBWP of broadly tuned membranes have not been investigated.

## 2 Shunt peaking by a voltage-dependent $K^+$ conductance

---

<sup>1</sup> Current address: Department of Bioengineering, Imperial College, London SW7 2AZ, UK

This is the author's final version. The version of record may be found at <https://doi.org/10.1098/rsif.2016.0719>. Please cite as Heras, Francisco J H, Laughlin, Simon B and Niven, Jeremy E (2016) *Shunt peaking in neural membranes*. *Interface*, 13 (124).

<sup>34</sup> To demonstrate that a conductance's inductive-like effects increases the GBPW by shunt peaking, thereby <sup>35</sup> increasing bandwidth without sacrificing gain, we modelled blowfly photoreceptors (Figure 1a-c). These

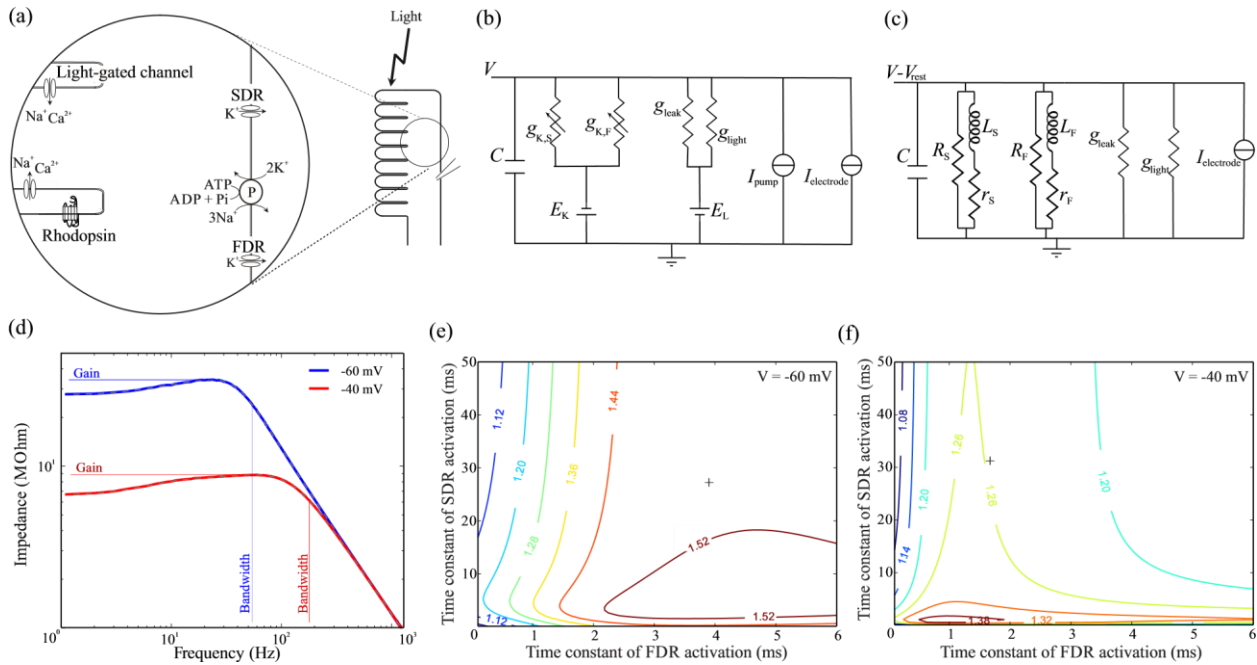


Figure 1: The fast delayed rectifier (FDR) produces shunt peaking in blowfly R1-6 photoreceptor membranes. (a) Schematic photoreceptor and inset showing the position of major components used to generate voltage responses to light. (b) Literal electrical (Hodgkin-Huxley) circuit model of the photoreceptor membrane. Capacitance,  $C$ , light-induced conductance,  $g_{light}$ , voltage-independent leak conductance,  $g_{leak}$ , fast and slow delayed rectifier conductances (FDR and SDR),  $g_{K,F}$  and  $g_{K,S}$ , and reversal potentials  $E_L$  and  $E_K$ . The  $Na^+/K^+$  ATPase generates pump current,  $I_p$ . (c) Phenomenological electrical circuit (RrLC) describes small signal behaviour of photoreceptor membrane to current injected around steady-state voltage,  $V_0$ , with SDR and FDR modelled as inductive elements. (d) Dark-adapted and light-adapted impedances of model blowfly photoreceptor calculated using responses to injected white noise current of low power (1pA std, 1kHz cut-off frequency) in the model depicted in (b). Superimposed grey dashed line is the impedance obtained using the equivalent RrLC circuit depicted in (c). Bandwidth and (maximum) gain used to calculate GBPW are shown. (e) Relative GBPW of dark-adapted photoreceptor depends on activation time constants of FDR and SDR. Black crosses indicate experimentally determined time constants [14]. (f) As in (e) but for the light-adapted photoreceptor.

<sup>36</sup> neurons transmit the signals produced by the fastest known G-protein biochemical cascade [11], but their <sup>37</sup> membrane capacitance is inflated by thousands of microvilli that capture and transduce photons. Reducing <sup>38</sup> the number and size of these microvilli to decrease capacitance would, however, impair performance by <sup>39</sup> reducing quantum catch and increasing noise [12, 13].

<sup>40</sup> The microvilli contain the components of the phototransduction cascade, including the visual pigment <sup>41</sup> and the depolarising light-gated channels [11]. The resulting inward light-induced current produces graded <sup>42</sup> changes in photoreceptor membrane potential, shaped by voltage-dependent channels in the light-insensitive <sup>43</sup> membrane [15]. Blowfly photoreceptors express two non-inactivating voltage-dependent  $K^+$  conductances, <sup>44</sup> the fast and the slow delayed

This is the author's final version. The version of record may be found at <https://doi.org/10.1098/rsif.2016.0719>. Please cite as Heras, Francisco J H, Laughlin, Simon B and Niven, Jeremy E (2016) *Shunt peaking in neural membranes*. *Interface*, 13 (124).

rectifier (FDR and SDR, Figure 1a,b). We model the conductance of both FDR and SDR with the formula  $g = \bar{g}m$ , where  $\bar{g}$  is the maximum conductance,  $m$  is a variable with steady state  $m_{\infty}(V)$ , time constant  $\tau$  and that changes with time and voltage according to the Hodgkin-Huxley equation [9]:

$$\frac{dm}{dt} = \frac{m_{\infty}(V) - m}{\tau} \quad (1)$$

Both DRs increase their steady-state conductance as the dark-adapted photoreceptor depolarises from its dark-adapted membrane potential of  $-60\text{mV}$  [14]. We simulated a photoreceptor membrane adapted to bright light by increasing the light conductance to produce membrane potential of  $-40\text{mV}$  (Supplementary

Material).

To determine the blowfly photoreceptor membrane GBWP, we obtained a closed formula for its impedance using small signal equivalent circuits for both FDR and SDR, each composed of a resistance  $R$  in parallel with a branch of a resistance  $r$  and an inductance  $L$  in series [1]

$$R = \frac{1}{\bar{g} m_{\infty}} \quad (2a)$$

$$r = \frac{1}{(V - E_K) \frac{d}{dV} (1/R)} \quad (2b) \quad L = \tau r \quad (2c)$$

55

Together with the voltage-independent leak conductance and the capacitance,  $C$ , they form the equivalent RrLC circuit of the photoreceptor membrane (Figure 1c). This circuit represents the linearisation around a steady state of the (non-linear) photoreceptor membrane, and gives a closed formula for the membrane impedance (Supplementary Material). As expected [1], the linearised model exactly reproduces the impedance estimated using the literal Hodgkin-Huxley model (Supplementary Material; Figure 1).

The impedance gain functions thus obtained are band-pass (Figure 1d). Calculating  $Q$ , the ratio between maximum and DC impedances (e.g. [16]), shows that the band-pass is less pronounced in the dark-adapted membrane ( $Q = 1.24$ ) than in the light-adapted membrane ( $Q = 1.34\sqrt{}$ ). At such low  $Q$  values, the GBWP is

the maximum (peak) gain times the frequency where gain falls to  $1/2$  ( $\sim 3$  dB) of the maximum (Figure 1d). The GBWP of the membrane is  $1846\text{M}\Omega\text{Hz}$  when dark-adapted and  $1538\text{M}\Omega\text{Hz}$  when light-adapted. By comparison, the GBWP of a passive membrane with the same capacitance but whose conductances are voltage-independent is  $1224\text{M}\Omega\text{Hz}$ . Thus, the inductive elements introduced by the DRs increase the membrane's GBWP by 51% when dark-adapted, and 26% when light-adapted, thereby demonstrating shunt

peaking.

The relative GBWP, the GBWP of the active membrane divided by that of a passive membrane with the same capacitance, changes with the DR activation time constants,  $\tau_F$  and  $\tau_S$  (Figure 1e,f), because the inductive elements producing shunt peaking are proportional to these time constants (Equation 2). For both dark-adapted and light-adapted membranes there is a time constant that optimizes the GBWP. For a dark-adapted membrane, the optimal relative GBWP is 1.56 (i.e. an improvement of 56% compared to the passive membrane), obtained when the FDR and SDR activation time constants are both 4.1 ms (Figure 1e), though a broad range of time constants have relative GBWP above 1.5 (Figure 1e). For a light-adapted membrane, the optimal relative GBWP is 1.41, obtained when both time constants are 0.89 ms (Figure 1f). The optimal time constants are remarkably similar to the measured activation time constant of the FDR (4.1 vs 3.9 ms and 0.89 vs 1.7 ms), but are substantially faster than those of the

This is the author's final version. The version of record may be found at <https://doi.org/10.1098/rsif.2016.0719>. Please cite as Heras, Francisco J H, Laughlin, Simon B and Niven, Jeremy E (2016) *Shunt peaking in neural membranes*. *Interface*, 13 (124).

SDR (4.1 vs 27 ms<sup>80</sup> and 0.89 vs 31 ms) [14]. This suggests that FDR activation times may be optimised for shunt peaking.<sup>81</sup> Furthermore, most of the shunt-peaking is produced by the FDR (see Supplementary Material). The SDR's<sup>82</sup> slower activation is more suited to decrease gain at low frequencies, contributing to the optimal filtering of<sup>83</sup> natural images in the presence of noise [17].

### 3 An inactivating voltage-dependent Na<sup>+</sup> conductance can produce

84

#### shunt peaking

85

<sup>86</sup> Many neural compartments supporting graded signalling express inward voltage-dependent Na<sup>+</sup> condu<sup>87</sup>ctances, as well as outward voltage-dependent K<sup>+</sup> conductances like those of blowfly photoreceptors. Voltage<sup>88</sup> dependent Na<sup>+</sup> conductances can produce membrane band passing through a resonance at specific frequen<sup>89</sup>cies, and are widespread in spiking neuron dendrites [1]. In honeybee drone photoreceptors voltage-dependent<sup>90</sup> Na<sup>+</sup> conductances selectively amplify the punctiform image of a queen moving across the sky [18]. We used<sup>91</sup> the Hodgkin-Huxley type model fitted by [18], which includes a voltage-dependent Na<sup>+</sup> conductance and<sup>92</sup> voltage-independent K<sup>+</sup> and light-induced conductances (Figure 2a). Using the corresponding RrLC cir<sup>93</sup>cuit (Figure 2b), we find a resonance, a prominent peak in the impedance ( $Q=3.19$ ), in the light-adapted<sup>94</sup> membrane (Figure 2c).

<sup>95</sup> This extreme band-passing –caused by the interaction of inductive elements representing inactivation and  
<sup>96</sup> the membrane capacitance– depends upon the inactivation time constant  $\tau_h$  of the voltage-dependent Na<sup>+</sup><sup>97</sup> conductance. A 10-fold increase in  $\tau_h$ , which is within biological limits [9], abolishes the resonance (Figure 2c).

<sup>98</sup> This leaves a low-passing ( $Q=1.04$ ) membrane in which the voltage-dependent Na<sup>+</sup> conductance produces<sup>99</sup> shunt peaking improving GBWP by  $\approx 50\%$ . By plotting relative GBWP as a function of the activation and<sup>100</sup> inactivation time constants ( $\tau_m$  and  $\tau_h$ , Figure 2d), we find a region where shunt peaking is produced (i.e.

<sup>101</sup> relative GBWP > 1), and a smaller region where that increase is produced while keeping a strictly low-pass<sup>102</sup> membrane. Thus, voltage-dependent Na<sup>+</sup> conductances can also produce shunt peaking, thereby improving<sup>103</sup> a membrane's GBWP.

### 4 Discussion

104

<sup>105</sup> Shunt peaking produced by the FDR increases GBWP of the dark and light-adapted blowfly photoreceptor<sup>106</sup> membrane, increasing membrane bandwidth whilst still permitting a high gain that reduces the effect of noise<sup>107</sup> at the photoreceptor outputs. In addition, the FDR reduces signal distortion by the photoreceptor mem<sup>108</sup>brane (Supplementary Materials), which is important for a wide-pass filter [6]. Shunt peaking achieves this<sup>109</sup> without incurring the deleterious effects of reducing the microvillar membrane area [13, 12], or compromising<sup>110</sup> membrane stability and minimum-phase (Supplementary Materials).

<sup>111</sup> Our approach it to linearise membrane responses around dark or light-adapted membrane potentials, but<sup>112</sup> when a blowfly photoreceptor scans a natural scene it frequently responds non-linearly to large fluctuations<sup>113</sup> in light intensity. However, DRs do not respond to light, they sense voltage and, because a photoreceptor's<sup>114</sup> mechanisms rapidly adjust gain, the DR's experience voltage fluctuations of standard deviation 2-7 mV<sup>115</sup> [19, Figure 5]. The linearized model of the light-adapted photoreceptor reproduces responses of even larger<sup>116</sup> amplitude of the Hodgkin-Huxley model to white noise current (data not shown) and should, therefore,<sup>117</sup> account for the DR's ability to improve the temporal resolution of the majority of signals. Improvements<sup>118</sup> are unlikely to cease when the membrane voltage responses exceed the limits of linearisation.

This is the author's final version. The version of record may be found at <https://doi.org/10.1098/rsif.2016.0719>. Please cite as Heras, Francisco J H, Laughlin, Simon B and Niven, Jeremy E (2016) *Shunt peaking in neural membranes*. *Interface*, 13 (124).

<sup>119</sup> Biological systems can escape the GWBP trap in other ways. As in electronic amplifiers [4], concatenating <sup>120</sup> several biochemical amplifiers multiplies gain but bandwidth remains close to the lowest bandwidth [20]. <sup>121</sup> However, the cost of such a strategy is energy and noise, produced and transmitted at every stage. Both <sup>122</sup> shunt-peaking and amplifier concatenation improve GBWP by increasing the number or the order of poles.

<sup>123</sup> By increasing GBWP without distorting the signal, shunt peaking may be particularly beneficial for <sup>124</sup> graded electrical signal transmission in neurons. Generally, an activating voltage-dependent conductance

<sup>125</sup> with a reversal potential below the resting potential or an inactivating voltage-dependent conductance with <sup>126</sup> a reversal potential above the resting potential can produce the inductive element needed to produce shunt

<sup>127</sup> peaking, provided that they have the correct time constant.

<sup>128</sup> Shunt peaking is unlikely to be restricted to fly photoreceptors. Hyperpolarisation-activated HCN chan<sup>129</sup> nels shape the graded voltage responses of rods and cones and, similar to blowfly photoreceptor, their effect <sup>130</sup> on small signals is well-described by a phenomenological inductance [21, 22]. HCN channels also act as <sup>131</sup> inductances in dendrites, and HCN channel blockers increases the apparent capacitance of hippocampal <sup>132</sup> neurons [16], suggesting that HCN channels implement shunt peaking. Dendritic membranes also contain <sup>133</sup> voltage-dependent  $K^+$  channels similar to blowfly photoreceptors', and voltage-dependent  $Na^+$  conductances <sup>134</sup> capable of producing sub-threshold resonances that selectively amplify particular frequencies [1]. Our anal<sup>135</sup> ysis of  $Na^+$  conductances in drone photoreceptors shows how resonance and shunt peaking can be generated <sup>136</sup> by the same mechanisms. Given that dendritic processing must achieve a minimum bandwidth without <sup>137</sup> reducing gain, shunt peaking could be widely employed by neurons.

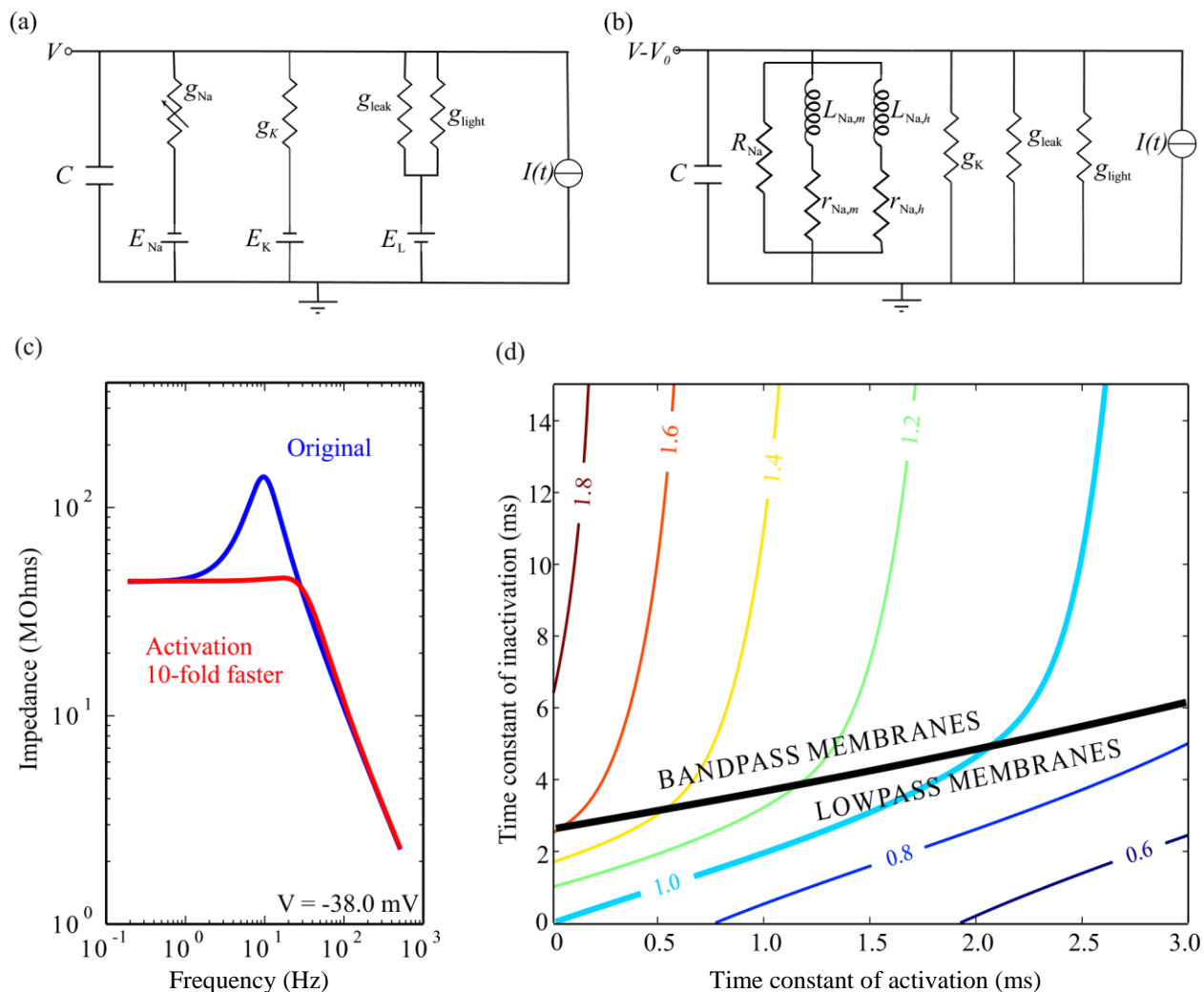


Figure 2: Inactivation of a  $\text{Na}^+$  conductance can produce shunt peaking. (a) Literal circuit model of drone bee photoreceptor. Membrane capacitance,  $C$ , light conductance,  $g_{\text{light}}$ , voltage-dependent  $\text{Na}^+$  conductance  $g_{\text{Na}}$ , and voltage-independent  $\text{K}^+$  conductance,  $g_{\text{K}}$ . Light current,  $\text{Na}^+$  current and  $\text{K}^+$  current reversal potentials are  $E_{\text{L}}$ ,  $E_{\text{Na}}$  and  $E_{\text{K}}$ , respectively. Leak conductance,  $g_{\text{leak}}$ , with reversal potential of light current, sets dark-adapted resting potential of photoreceptor. (b) Phenomenological RrLC circuit of the photoreceptor describing small signal behaviour of membrane to current injected around steady-state voltage,  $V_0$ . The voltage-dependent conductance  $g_{\text{Na}}$  is modelled as a resistance,  $R$ , in parallel with two phenomenological branches, representing the effect of activation ( $L_m, r_m$ ) and inactivation ( $L_h, r_h$ ), respectively. (c) Impedance of the model drone photoreceptor membrane (blue) and a modified membrane model with 10 times faster inactivation (red). (d) Relative GBWP of drone photoreceptor as function of activation and inactivation time constants of the voltage-dependent  $\text{Na}^+$  conductance. Thick black line marks the border between band-pass membranes and low-pass membranes.

### 138 Authors' contributions

139 F.J.H.H. conceived study, wrote code and conducted analyses. F.J.H.H. and J.E.N. wrote manuscript with 140 input from S.B.L. All authors gave final approval for publication.

This is the author's final version. The version of record may be found at <https://doi.org/10.1098/rsif.2016.0719>. Please cite as Heras, Francisco J H, Laughlin, Simon B and Niven, Jeremy E (2016) *Shunt peaking in neural membranes*. *Interface*, 13 (124).

## 141 Competing interests

142 We declare no competing interests.

## 143 Funding

144 This work was funded by Fundación Caja Madrid and Trinity College (F.J.H.H.) and Royal Society (J.E.N.).

## 145 References

- 146 [1] Koch, C., 1999. *Biophysics of Computation: Information Processing in Single Neurons*. Oxford University Press, USA.
- 148 [2] Gentet, L. J., Stuart, G. J. & Clements, J. D., 2000. Direct measurement of specific membrane capacitance in neurons. *Biophys. J.* 79, 314–320.
- 150 [3] Sengupta, B., Faisal, A. A., Laughlin, S. B. & Niven, J. E., 2013. The effect of cell size and channel density on neuronal information encoding and energy efficiency. *J. Cereb. Blood Flow Metab.* 33, 1465–1473.
- 152 [4] Steininger, J., 1990. Understanding wide-band MOS transistors. *IEEE Circuit. Devic.* 6, 26–31.
- 153 [5] Wong, S. & Salama, A. T., 1983. Impact of scaling on MOS analog performance. *IEEE J. Solid-St. Circ.* 18, 106–114.
- 154 [6] Mohan, S., Hershenson, M., Boyd, S. & Lee, T., 2000. Bandwidth extension in CMOS with optimized on-chip inductors. *IEEE J. Solid-St. Circ.* 35, 346–355.
- 156 [7] Scott, A. C., 1971. Effect of the series inductance of a nerve axon upon its conduction velocity. *Math. Biosci.* 11, 277–290.
- 158 [8] Cole, K. S., 1941. Rectification and inductance in the squid giant axon. *J. Gen. Physiol.* 25, 29–51.
- 160 [9] Hodgkin, A. L. & Huxley, A. F., 1952. A quantitative description of membrane current and its application to conduction and excitation in nerve. *J. Physiol.* 117, 500–544.
- 161 [10] Mauro, A., 1961. Anomalous impedance, a phenomenological property of time-variant resistance: An analytic review. *Biophys. J.* 1, 353–372.
- 163 [11] Hardie, R. C., 2012. Phototransduction mechanisms in drosophila microvillar photoreceptors. *WIREs Membr. Transp. Signal* 1, 162–187.
- 165 [12] Snyder, A. W., 1977. Acuity of compound eyes: Physical limitations and design. *J. Comp. Physiol.* 116, 161–182.
- 167 [13] Anderson, J. C. & Laughlin, S. B., 2000. Photoreceptor performance and the co-ordination of achromatic and chromatic inputs in the fly visual system. *Vis. Res.* 40, 13–31.
- 169 [14] Weckström, M., Hardie, R. C. & Laughlin, S. B., 1991. Voltage-activated potassium channels in blowfly photoreceptors and their role in light adaptation. *J. Physiol.* 440, 635–657.

This is the author's final version. The version of record may be found at <https://doi.org/10.1098/rsif.2016.0719>. Please cite as Heras, Francisco J H, Laughlin, Simon B and Niven, Jeremy E (2016) *Shunt peaking in neural membranes*. *Interface*, 13 (124).

- <sup>173</sup> [15] Weckström, M. & Laughlin, S. B., 1995. Visual ecology and voltage-gated ion channels in insect photoreceptors. *Trends Neurosci.* 18, 17–21.
- <sup>175</sup> [16] Zemankovics, R., Káli, S., Paulsen, O., Freund, T. F. & Hájos, N., 2010. Differences in subthreshold resonance of hippocampal pyramidal cells and interneurons: the role of h-current and passive membrane characteristics. *J. Physiol.* 588, 2109–2132.
- <sup>178</sup> [17] van Hateren, J. H., 1992. Theoretical predictions of spatiotemporal receptive fields of fly LMCs, and experimental validation. *J. Comp. Physiol. A* 171, 157–170.
- <sup>180</sup> [18] Vallet, A. M., Coles, J. A., Eilbeck, J. C. & Scott, A. C., 1992. Membrane conductances involved in amplification of small signals by sodium channels in photoreceptors of drone honey bee. *J. Physiol.* 456, 303–324.
- <sup>183</sup> [19] van Hateren, J. H., 1997. Processing of natural time series of intensities by the visual system of the blowfly. *Vis. Res.* 37, 3407–3416.
- <sup>185</sup> [20] Detwiler, P. B., Ramanathan, S., Sengupta, A. & Shraiman, B. I., 2000. Engineering aspects of enzymatic signal transduction: Photoreceptors in the retina. *Biophys. J.* 79, 2801–2817.
- <sup>187</sup> [21] Demontis, G. C., Longoni, B., Barcaro, U. & Cervetto, L., 1999. Properties and functional roles of hyperpolarization-gated currents in guinea-pig retinal rods. *J. Physiol.* 515, 813–828.
- <sup>189</sup> [22] Barrow, A. J. & Wu, S. M., 2009. Low-conductance HCN1 ion channels augment the frequency response of rod and cone photoreceptors. *J. Neurosci.* 29, 5841–5853.